Polymer Chemistry

Accepted Manuscript

ROYAL SOCIETY OF CHEMISTRY

www.rsc.org/polymers

Polymer Chemistry

Cite this: DOI: 10.1039/c0xx00000x

www.rsc.org/xxxxxx

Full Paper

Stimulus Responsive Cross-linked AIE-active polymeric Nanoprobes: Fabrication and Biological Imaging Application

Qing Wan[a], Ke Wang[b], Chengbin He[a], Meiying Liu[a], Guangjian Zeng[a], Hongye Huang[a], Fengjie Deng[a], Xiaoyong Zhang[a,*], and Yen Wei[b,*]

Received (in XXX, XXX) Xth XXXXXXXXX 200X, Accepted Xth XXXXXXXXX 200X

DOI: 10.1039/b000000x

The combination of functional polymers and hydrophobic AIE dyes to prepare luminescent organic nanoparticles (LONs) with strong fluorescence, great water dispersibility and desirable biocompatibility have received numerous attentions for their potential applications in cell imaging and theranostics. Although great effort has been devoted to preparing AIE dye based LONs through both covalent and noncovalent strategies, the fabrication of cross-linked AIE dye based LONs with stimulus responsive behavior has not been reported previously. In this work, the AIE dye based LONs were constructed via cross-linking aldehyde-containing polymers and AIE dye (2,2'-diaminotetraphenyl ethylene) with two amino groups through formation of Schiff base, which is a well known dynamic bond with pH responsiveness. After successful incorporation of the hydrophobic AIE dye into the copolymers, cross-linked core-shell lunminescent nanoparticles can be formed. The obtained AIE dye based LONs exhibited strong fluorescence and high water dispersiblity because the AIE dye was aggregated in the core and the hydrophilic polymers were covered on the shell. Biological evaluation results demonstrated that the AIE dye based LONs exhibited excllent biocompatibility and biological imaging properties. More importantly, these AIE dye based LONs exhibited desirable pH responsiveness, implied that these polymeric LONs are potentially utilized for pH sensor and controlled drug delivery. Combination of the dynamic crosslinking and pH responsiveness, the obtained AIE dye based LONs should be of great significance for biomedical application.

1. Introduction

Fluorescent polymers, that can self assemble into luminescent organic nanoparticles (LONs) have been extensively investigated in the past few decades for biomedical applications because of their well designability, excellent biocompatibility, biodegradable and multifunctional potential.[1-8] These luminescent polymers have demonstrated to possess some obvious advantages as compared with the fluorescent inorganic nanoparticles (FINs) and fluorescent proteins.[9-14] The LONs can effectively overcome the toxicity and nonbiodegradability of FINs, and the high cost and photobleahcing of fluorescent proteins.[11, 15-20] The basic principle for fabrication of LONs is relied on the formation of amphiphilic dyes contained micelles, which could passively accumulate in the tumor sites.[21-23] After self assembly, the hydrophobic dyes were encapsulated in the core of micelles, while the hydrophilic segments of the LONs were extended in water as the shell, which could render the excellent water dispersibility and biocompatibility of LONs.[24, 25] However, fabrication of LONs with desirable fluorescent properties using conventional organic dyes is still challenging due to the aggregation of dyes in the core of LONs, which will obviously decrease the fluorescence of LONs. It is also known as aggregation caused quenching (ACQ) effect.

Aggregation induced emission (AIE) materials were first reported by Tang and co-workers in 2001.[26] In contrast with the conventional organic dyes, the AIE active dyes can emit much strong fluorescence in high concentration and solid state. The unique AIE feature provided an elegant route to overcome the notorious ACQ effect.[21, 27] Since the first report of AIE phenomenon by Tang's group, a number of novel dyes with typical AIE characterization such as siloles,[28-31] triphenylethene,[32-34] cyano-substituted diarylethene,[35-38] distyrylanthracene derivatives,[39, 40] and phenothiazine[41, 42] were synthesized. And different fabrication strategies such as noncovalent self assembly, covalent conjugation and polymerization have been established to fabricate of AIE active polymeric nanoprobes.[39, 43-54] On the one hand, these polymeric AIE active nanoprobes could effectively overcome the poor water dispersibility of AIE dyes. On the other hand, many other functional groups can be integrated into these polymeric nanoprobes, which can extend largely their applicability for biological sensor and therapeutics.[50-52, 55, 56] For example, Li and co-workers have developed a novel method for the fabrication of cross-linked AIE active polymeric nanoprobes through combination of living radical copolymerization of 2-isocyanatoethyl methacrylate and poly(ethylene glycol)

monomethyl ether methacylate. And then the obtained copolymers were subsquently cross-linked by AIE dyes with two amino groups.[57] More recently, our group has fabricated cross-linked PEGylated AIE active nanoprobes take advantage of the different reaction activity between anhydride and chloride of Trimellitic anhydride chloride, which was served as the linker between the amino-terminated AIE dye and the hydroxyl group of PEG.[58] However, there are still some problems existed in these polymeric nanosystems, which included poor solution stability at low concentration and lack of responsiveness. Therefore, the fabrication of cross-linked stimulus responsive AIE active polymeric nanosystems is expected to overcome of these drawbacks. However, to the best of our knowledge, such cross-linked AIE active polymeric nanoprobes with stimulus responsiveness have not been fabricated thus far.

In this contribution, novel cross-linked AIE active polymeric LONs (DATPE-poly(PEGMA-co-HEA) LONs) with pH responsiveness have been facilely fabricated for the first time through formation of Schiff base. As shown in S**cheme 1**, the aldehyde-containing polymers AD-poly(PEGMA-co-HEA) were synthesized via conjugation of benzaldehyde with poly(PEGMA-co-HEA), which were obtained by living radical polymerization (LRP) using poly(ethylene glycol) methyl methacrylate (PEGMA) and hydroxyl-contained monomer 2-Hydroxyethyl acrylate (HEA) as the monomers and 2,2'-azobisisobutyronitrile (AIBN) as initiator. The successful formation of these AIE-active polymeric nanoprobes was confirmed by various characterization techniques. Our results suggested that these AIE active LONs emit strong fluorescence and excellent water dispersibility in pure aqueous solution for the AIE feature of TPE dyes and the amphiphilic properties of these obtained polymers. More importantly, due to formation of Schiff base, the fluorescence emission of the obtained polymeric LONs was obvious red shift as compared with the DATPE and showed pH responsiveness. Furthermore, cell experimental results suggested that DATPE-poly(PEGMA-co-HEA) LONs are well biocompatible with cells and can be utilized for cell imaging applications. Given their good water dispersibility, desirable biocompatibility and pH responsiveness, DATPE-poly(PEGMA-co-HEA) LONs should be promising candidates for biological imaging and controlled drug delivery.

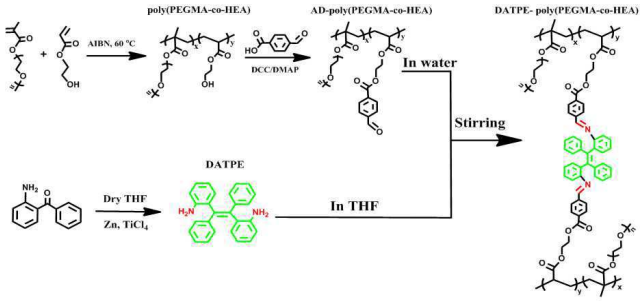

Scheme 1. The schematic showing the synthesis of hydrophilic functional polymers (AD-poly(PEGMA-co-HEA)), AIE dye (DATPE) and pH responsive cross-linked AIE active DATPE-poly(PEGMA-co-HEA) LONs.

2. Experiments

2.1 Materials and Characterization

All chemicals were of analytical grade and were used as received without any further purification. The other experimental chemical substances such as Zinc powders, titanium tetrachloride, 2-Aminobenzophenone (MW:197.23, 99.0%) and anhydrous THF were provided from Heowns (Tianjin, China), ammonium chloride and ethyl acetate solution were supplied from Sinopharm Chemical reagents Co., Ltd. (Shanghai, China). The monomer poly(ethylene glycol) methyl methacrylate (MW: 950, 98%) and 2-Hydroxyethyl acrylate (MW: 116.12, 96%) were used to synthesize hydroxyl-contained copolymer (poly(PEGMA-co-HEA)), which were supplied from Aladdin company (Shanghai China). N,N'-Dicyclohexylcarbodiimide (DCC, MW:206.33, 99.0%), 4-Dimethylaminopyridine (DMAP, MW: 122.17, 99.0%) and 4-Carboxybenzaldehyde (MW:150.13, 99.8%) were also purchased from Aladdin company. DATPE was synthesized using the method as described in our previous report.[58]

^{1}H NMR spectra were recorded on Bruker Avance-400 spectrometer with D_2O and $CDCl_3$ as the solvents. The synthesized polymers and materials were characterized by Fourier transform infrared spectroscopy (FT-IR) using KBr pellets, The FT-IR spectra were supplied from Nicolet5700 (Thermo Nicolet corporation). The transmission electron microscopy (TEM) specimens were got by putting a drop of the nanoparticle ethanol suspension on a carbon-coated copper grid. TEM images were recorded on a Hitachi 7650B microscope operated at 80 kV. The fluorescence data were obtained from the Fluorescence spectrophotometer (FSP, model: C11367-11), which was purchased from Hamamatsu (Japanese).

2.2 Synthesis of poly(PEGMA-co-HEA) and AD-poly(PEGMA-co-HEA)

The hydrophilic copolymers (poly(PEGMA-co-HEA)) were prepared using poly(ethylene glycol) methyl methacrylate (PEGMA) and 2-Hydroxyethyl acrylate (HEA) as monomers via LRP. The procedure could be clearly described as follows: the moisture of PEGMA was removed by using toluene as water-carrying solvent by rotary evaporation method before reaction. The mixture of PEGMA (3.04 g, 3.2 mM) and HEA (46 mg, 0.4 mM) were dissolved in dry ethyl acetate (20 mL) and put into polymerization bottle under N_2 atmosphere. After acutely stirring at 60 °C for 10 min, the AIBN powders (50 mg) were dissolved in anhydrous ethyl acetate (1 mL) and injected into reactive system. After 24 h, the white solid copolymer (poly(PEGMA-co-HEA)) could be obtained after reactive mixture cooled at room temperature and participated using cooled anhydrous diethyl ether. The white solid powders were dried at vacuum for further characterization and reaction. The aldehyde-functional poly(PEGMA-co-HEA) copolymers were also prepared for further fabrication of hydrophilic LONs based on unique AIE dyes. Using synthesized poly(PEGMA-co-HEA) and purchased 4-Carboxybenzaldehyde as reaction substrates, the AD-poly(PEGMA-co-HEA) could be facilely prepared by dehydration procedure based on DCC/DMAP system at room temperature for 18 h. Poly(PEGMA-co-HEA) (500 mg), 4-Carboxybenzaldehyde (500 mg) and DMAP (50 mg) were dissolved in dry THF solution, followed by the addition of DCC (800 mg) under N_2 atmosphere. After reaction completing, the resulting AD-poly(PEGMA-co-HEA) products would be received when the mixture were precipitated with cool dry diethyl ether

and suction filtration. Thus obtained crude products were purified with repeatedly dissolved in THF and precipitated in dry diethyl ether for three times for further characterization and application.

2.3 The fabrication of DATPE-poly(PEGMA-co-HEA) LONs

The design of uniform morphology and controlled size at nanoscale is special important for various applications of fluorescent AIE active polymeric materials such as bioimaging and drug delivery. The cross-linked AIE active LONs with pH responsiveness were prepared via formation of Schiff base. In brief, AD-poly(PEGMA-co-HEA) (300 mg) in distilled water (10 mL) and DATPE (60 mg) in THF (20 mL) were mixed and added 5 drops of trimethylamine (TEA), stirring at room temperature for 8 h. Following by the removal of THF and water by rotary evaporation. The crude products were washed with dry THF to remove residual DATPE. Thus obtained DATPE-poly(PEGMA-co-HEA) copolymers were dialyzed with pure water for 24 h and soaked in ethanol for 8 h using 3500 Da Mw cutoff dialysis tubes. The resulting products were dried at vacuum for further characterization and applications.

2.4 Cytotoxicity evaluation of DATPE-poly(PEGMA-co-HEA) LONs

The cell viability of DATPE-poly(PEGMA-co-HEA) LONs based on the DATPE dyes for HeLa cells was evaluated by cell counting kit-8 (CCK-8) assay.[59, 60] Briefly, cells were put into 96-well microplates at a density of 5×10^4 cells mL^{-1} in 160 μL of respective media containing 10% fetal bovine serum (FBS). After 24 h of cell attachment, the cells were incubated with 20-100 μg mL^{-1} LONs for 12 and 24 h. Then nanoparticles were removed and cells were washed with PBS three times. 10 μL of CCK-8 dye and 100 μL of DMEM cell culture medium were added to each well and incubated for 2 h at 37 °C. Afterward, plates were analyzed using a microplate reader (VictorIII, Perkin-Elmer). Measurements of formazan dye absorbance were carried out at 450 nm, with the reference wavelength at 620 nm. The values were proportional to the number of live cells. The percent reduction of CCK-8 dye was compared to controls (cells not be exposured to hydrophilic LONs), which represented 100% CCK-8 reduction. Three replicate wells were used per microplate, and the experiment was operated for three times. Cell survival was expressed as absorbance relative to that of untreated controls. Results are presented as mean ± standard deviation (SD)

2.5 Cell imaging application of DATPE-poly(PEGMA-co-HEA) LONs

HeLa cells were facilely bred in Dulbecco's modified eagle medium (DMEM), which was supplied with 10% heat-inactivated FBS, 2 mM glutamine, 100 U mL^{-1} penicillin, and 100 μg mL^{-1} of streptomycin. Before proceeding experiment of cell imaging, the cell culture should be controlled at 37 °C in a similar human environment of 95% air and 5% CO_2 in culture medium. In order to maintain the exponential growth of the cells, the culture medium should be updated every three days. Before treatment, cells were seeded in a glass bottom dish with a density of 1×10^5 cells per dish. On the day of treatment, the cells were incubated with DATPE-poly(PEGMA-co-HEA) dispersion liquid at a final concentration of 20 μg mL^{-1} for 3 h at 37 °C. Afterward, the cells were washed three times with PBS to remove the DATPE-poly(PEGMA-co-HEA) LONs and then fixed with 4% paraformaldehyde for 10 min at room temperature. Cell images were obtained using a confocal laser scanning microscope (CLSM) Zesis 710 3-channel (Zesis, Germany) with the excitation wavelength of 405 nm.

3. Results and discussion

The fabrication of water soluble, biocompatible LONs with outstand optical properties has attracting great attention recently. AIE-active dyes have been considered as the most promising candidates for fabrication of such LONs for their unique AIE feature, which could elegantly overcome the ACQ effect of conventional organic dyes. Although a number of strategies have been developed for fabrication of AIE-active LONs previously. The cross-linked AIE-active LONs with pH responsiveness have not reported before. In this work, synthesized functional polymers (AD-poly(PEGMA-co-HEA)) with pendant aldehyde groups were synthesized by combination of LRP and esterification reaction, and then the amino-contained AIE dye (DA-TPE) was served as the cross-linker to react with AD-poly(PEGMA-co-HEA) through formation of Schiff base.

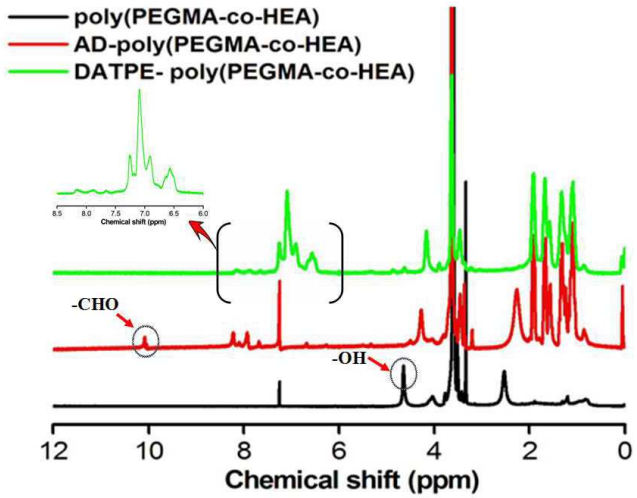

Fig. 1 The ^{1}H NMR spectra of poly(PEGMA-co-HEA), AD-poly(PEGMA-co-HEA) and DATPE- poly(PEGMA-co-HEA). It can be seen that the multiplet of signal at 4.65 ppm corresponding to the hydroxyl groups was disapeared after the esterification reaction. On the other hand, the signal with chemical shift at 10.12 ppm was emerged in AD-poly(PEGMA-co-HEA). These results demonstrated that the aldehyde contained polymers have been successfully synthesized. Moreover, the peaks between 6.0 and 8.5 ppm was found in the sample DATPE-poly(PEGMA-co-HEA). These ^{1}H NMR peaks can be attributed to the aromatic ring of DATPE. Therefore, the ^{1}H NMR spectra confirmed that DATPE has successfully reacted with AD-poly(PEGMA-co-HEA) through formation of Schiff base.

The ^{1}H NMR spectra gave the clear evidence that successful preparation of poly(PEGMA-co-HEA), AD-poly(PEGMA-co-HEA) and DATPE-poly(PEGMA-co-HEA). As shown in **Fig. 1**, among the samples of poly(PEGMA-co-HEA) and AD-poly(PEGMA-co-HEA), the disappearance of multiplet at 4.65 ppm (-OH) of poly(PEGMA-co-HEA) and appearance of single peak at 10.12 ppm (-CHO) of AD-poly(PEGMA-co-HEA) suggested the successful conjugation of 4-Carboxybenzaldehyde

with poly(PEGMA-co-HEA). Furthermore, a series of peaks located between 7.0 and 8.5 ppm were firstly appeared, which indicated the introduction of benzene rings, providing powerful evidence that successful preparation of AD-poly(PEGMA-co-HEA) through esterification reaction. Furthermore, the chemical shift at 10.12 ppm was vanished in the ^{1}H NMR spectrum of DATPE-poly(PEGMA-co-HEA). The disappearance of aldehyde signal clearly demonstrated the successful formation of Schiff base between AIE dyes and AD-poly(PEGMA-co-HEA). More importantly, the intensity of peaks between 6.0 and 8.5 ppm are obviously enhanced in the sample of DATPE-poly(PEGMA-co-HEA) as compared with AD-poly(PEGMA-co-HEA). It implied that more benzene rings have been contained in DATPE-poly(PEGMA-co-HEA). Therefore, it can be concluded that successful fabrication of DATPE-poly(PEGMA-co-HEA) LONs based on ^{1}H NMR spectra.

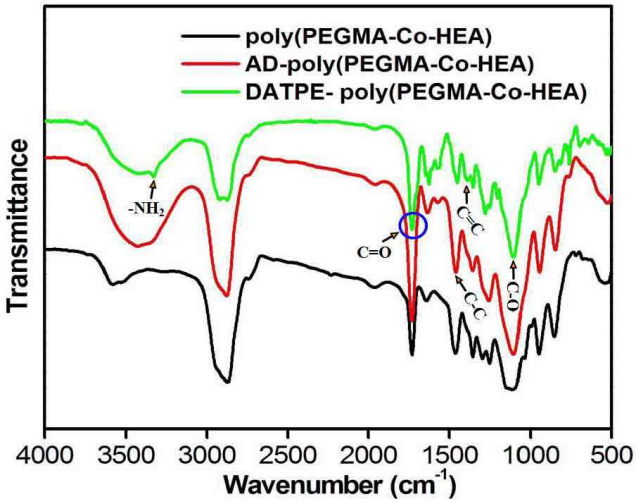

Fig. 2 FT-IR spectra of poly(PEGMA-co-HEA), AD-poly(PEGMA-co-HEA) and DATPE-poly(PEGMA-co-HEA). The characteristic peaks at 1108, 1732, 2840, 3620 cm^{-1} were found in poly(PEGMA-co-HEA), implied that the successful preparation of polymers with C-O, C=O, -CH_3 and –OH. After formation of AD-poly(PEGMA-co-HEA) and DATPE-poly(PEGMA-co-HEA), the intensity of peak at 1732 cm^{-1} was obviously enhanced, suggesting that the 4-Carboxybenzaldehyde and DATPE have conjugated with poly(PEGMA-co-HEA).

The FT-IR spectra of poly(PEGMA-co-HEA), AD-poly(PEGMA-co-HEA) and DATPE-poly(PEGMA-co-HEA) were displayed in **Fig. 2**. As compared with poly(PEGMA-co-HEA), the signal of peak at 1732 cm^{-1} (attributed to the stretching vibration of C=O) was enhanced, which could be explained the introduction of more ester bonds via esterification reaction between poly(PEGMA-co-HEA) and 4-Carboxybenzaldehyde. On the other hand, a weak peak at 1580 cm^{-1} attributed to the stretching vibration of –CHO was observed, further suggesting the successful preparation of AD-poly(PEGMA-co-HEA). Futhermore, the weak peak at 3340 assigned to the stretching vibration of N-H were found in the sample DATPE-poly(PEGMA-co-HEA). Furthermore, these are some tanglesome peaks appeared at ranging 500 to 1000 cm^{-1}, which can be defined as fingerprint region of benzene rings. These results proved that DATPE was conjugated with AD-poly(PEGMA-co-HEA) via typical Schiff base reaction. Due to the hydrophilicity of PEGMA and the hydrophobicity of DATPE, thus obtained copolymers should be amphiphilic, whihc are prone to self assemble into core-shell polymeric nanoparticles in pure aqueous solution. In the nanoparticles, the hydrophobic AIE dye (DATPE) will be encapsulated in the core, while the hydrophilic PEG will be extended into water and served as the shell. It is therefore, the polymeric nanoparticles are expected to emit strong fluorescence and show well water dispersibility due to the aggregation of AIE dye. As shown in the inset of **Fig. 3,** uniform water suspension can be obtained through direct dispersion of DATPE-poly(PEGMA-co-HEA) in pure water. Strong green fluorescence can be observed after DATPE-poly(PEGMA-co-HEA) water suspension was irradiated by UV lamp at 365 nm. These results further evidenced the successful formation of DATPE-poly(PEGMA-co-HEA) LONs through Schiff base reaction.

The optical properties of DATPE-poly(PEGMA-co-HEA) LONs were investigated by UV-Vis spectroscopy and fluorescent spectroscopy. As shown in **Fig. S1**, two major absorption peaks at 333 nm and 386 nm were found in UV-Vis spectrum. Among them, the adsorption peak at 386 nm can be ascribed to the n-π* transitions. While the peak at 333 nm should be attributed to a singlet–singlet π–π* transition. Furthermore, the absorption peak of polymeric nanoparticles at 386 nm was almost closed to excitation wavelength (408 nm), suggesting that fluorescent cross-linked nanoparticles between hydrophilic polymers and hydrophobic AIE dye could disperse uniformly in aqueous solution. Well consistent with the optical images in **Fig. 3**, the max emission peak of DATPE-poly(PEGMA-co-HEA) LONs was at the position of 496 nm when they were excitated with wavelength at 365 nm. While the optimal fluorescent excitation wavelength was located at 408 nm using the 496 nm as the emission peak. As compared with the fluorescent spectra of TPE-NH_2, the excitation and emission peaks of DATPE-poly(PEGMA-co-HEA) LONs were obvious red shift. The red shift of excitation and emission peaks is likely due to the formation of Schiff base, which could increase the conjugation plane of DA-TPE. On the other hand, DATPE-poly(PEGMA-co-HEA) LONs exhibited excellent photostability. After irradiated by UV lamp at 365 nm for 30 min, the fluorescent intensity of DATPE-poly(PEGMA-co-HEA) LONs showed almost no difference (**Fig. S2**). The excellent photostability is very useful for biological imaging especially for long-term imaging or two-photon biological imaging because of the photobleaching of small organic dye. The fluroescent quantum yield (QY) is another important parameter, which is critical for the biological imaging application. In this work, we have examined the QY using quinine sulfate as the reference dye. Our results suggested that the QY of DATPE-poly(PEGMA-co-HEA) LONs is as high as 19.3%. These remarkable fluorescent properties of DATPE-poly(PEGMA-co-HEA) LONs make them be promising candidates for biological applications.

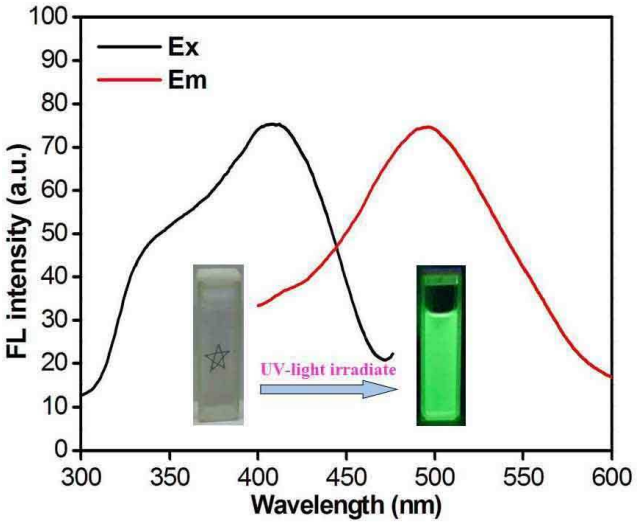

Fig. 3 The fluorescent excitation and emission spectra of DATPE-poly(PEGMA-co-HEA) dispersed in water. The inset at the left is DATPE-poly(PEGMA-co-HEA) directly dispersed in pure water (regarding "star" as background to show great dispersibility of LONs in water), the right inset with strong green fluorescence of LONs in water when they were irradiated by UV lamp at 365 nm. The fluorescent spectra of DATPE-poly(PEGMA-co-HEA) LONs are well consistent with the optical images. It can be seen that the maxmium emission peak of DATPE-poly(PEGMA-co-HEA) LONs is located at 496 nm when they were excitated at the wavelength of 365 nm.

It is well known that the Schiff base can be responsed to the pH.[61, 62] As the pH decreased to a critical value, the Schiff base will be degraded into amino and aldehyde groups. Over the past few decades, the pH responsiveness of Schiff base has attracted great research attention and widely explored for fabrication of responsive materials for different biomedical applications, e.g. pH responsive drug delivery carriers.[61] To the best of our knowledge, the pH responsive AIE active polymeric nanoprobes has not fully investigated. Herein, pH responsiveness of DATPE-poly(PEGMA-co-HEA) LONs was detailedly investigated using fluorescent spectroscopy. As shown in **Fig. 4**, the maximum emission peak of DATPE-poly(PEGMA-co-HEA) LONs was located at 496 nm when the pH values of solutions are 9.4 and 7.4, and the fluorescent intensity of DATPE-poly(PEGMA-co-HEA) LONs showed only little difference. However, when the pH value of solution decreased to 5.0, the emission peak was shifted to 481 nm, indicating that Schiff base in DATPE-poly(PEGMA-co-HEA) LONs was destroyed in acid environment. When the pH value was further decreased to 3.2, the emission peak was located at 472 nm. Moreover, the fluorescent intensity of DATPE-poly(PEGMA-co-HEA) LONs was significantly decreased. These results suggested that AIE dye was completely detached from the polymers, which resulted in the qucik precipitation of AIE dye (**Fig. S3**). All of the above results clearly demonstrated that the DATPE-poly(PEGMA-co-HEA) LONs possess desirable pH responsiveness, which should be useful for design pH sensor and drug delivery systems.

Due to their amphiphilic properties of DATPE-poly(PEGMA-co-HEA), these copolymers are tended to self assemble into nanoparticles, in which the hydrophobic AIE active dye was encapsulated in their core, while the hydrophilic PEGMA was covered on the shell. It is therefore DATPE-poly(PEGMA-co-HEA) LONs showed strong flurorescence and high water dispersibility due to their self assembly. The size and morphology of DATPE-poly(PEGMA-co-HEA) LONs were characterized by TEM. It can be seen that uniform spherical nanoparticles with size ranged from 100-300 nm can be observed (**Fig. S4**). The size distribution of DATPE-poly(PEGMA-co-HEA) LONs based on TEM images was calculated to be 223 ± 31 nm. Furthermore, the hydrodynamic size distribution of DATPE-poly(PEGMA-co-HEA) LONs was determined by dynamic light scattering (DLS) measurement. Our results suggested that the size of DATPE-poly(PEGMA-co-HEA) LONs in deionized water and phosphate buffer solution (PBS) is 385.3 ± 35.2 and 426.4 ± 45.6 nm, respectively. As compared with the TEM characterization, the size distribution of DATPE-poly(PEGMA-co-HEA) LONs determined by DLS is relativly large, which should be attributed to the shrinkage of polymeric nanoparticles for TEM characterization.

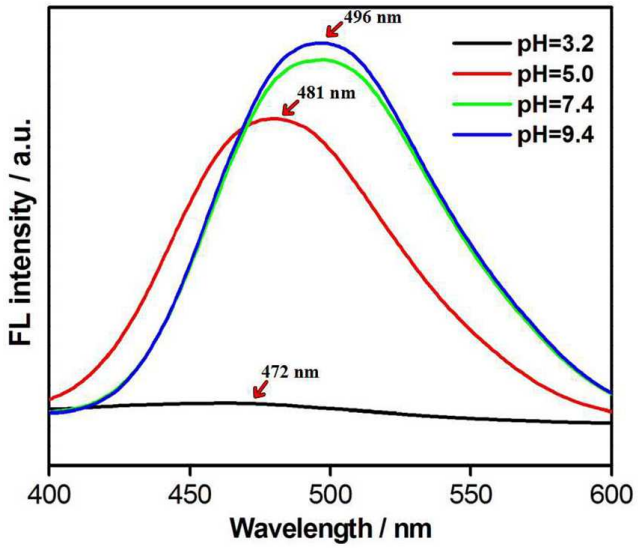

Fig. 4 The FL spectra of DATPE- poly(PEGMA-co-HEA) cross-linked materials were respectively dispersed in aqueous solution with different pH system, which was used to verify that successful formation of Schiff base bond.

As a promising biomaterial, the excellent biocompatibility is one of the most important requirement.[63, 64] In this work, the preliminary biocompatibility of DATPE-poly(PEGMA-co-HEA) LONs with living cells was examined by the cell counting kit-8 (CCK-8) assay. As shown in **Fig. S5**, cell viability values don't significantly decreased after HeLa cells were incubated with different concentrations of polymeric LONs (20-100 μg mL^{-1}) for 12 and 24 h. Furthermore, when the incubated concentration of LONs arrived to the 100 μg mL^{-1}, the cell viability was still more than 94%. These results confirmed that DATPE-poly(PEGMA-co-HEA) LONs possess great cytocompatibility. Considered the uniform nanoscale size, intense fluorescence, great biocompatibility and water dispersibility, the cell imaging applications of DATPE-poly(PEGMA-co-HEA) LONs were further investigated using CLSM. As shown in **Fig. 5**, the HeLa cell uptake behavior for these AIE active LONs was evaluated by CLSM. It can be seen that cells still kept their normal morphology after incubated with DATPE-poly(PEGMA-co-HEA) LONs, further confirming the biocompatibility of these

polymeric LONs. On the other hand, even the concentration of DATPE-poly(PEGMA-co-HEA) LONs is 20 μg mL^{-1}, the cell uptake of these AIE active LONs can still be observed by CLSM. This should be attributed to the AIE properties of DATPE, which showed strong fluoresence in its aggregation state. Moveover, some black areas were around by the areas with strong green fluorescence. These black areas should be the locations of cell nucleus. Because these AIE active LONs have not surface modified with targeting agents, they should be uptaken by cells through the direct endocytosis route, which has been demonstrated to be the common way for cell uptake. This procedure has been suggested that dependent on the incubation temperature, structure characteristic of nanomaterials and the surface chemistry of nanoparticles.[65, 66] Therefore, we believe that DATPE-poly(PEGMA-co-HEA) LONs were entered into cells through endocytosis and mainly distributed in the cytoplasma. The Schiff base is a well known dynamic bond, which can be responsed to pH change. The Schiff base can degrade in acid environment and therefore is very useful for design biomaterials for controlled drug release applications.[62] In this work, the DATPE with two amino groups was served as the linker to fabricate cross-linked AIE active polymeric nanoprobes. As compared with the noncrosslinked ones, the dynamic crosslinked polymeric nanoprobes are expected to overcome the critical micelle concentration (CMC) of noncrosslinked nanoprobes. On the other hand, they also have some advantages for responsive cell imaging and drug delivery due to the pH responsiveness of Schiff base. Therefore, these dynamic crosslinked polymeric nanoprobes should be novel and more promising nanotheranostics for the AIE properties of dyes and pH responsiveness of Schiff base.

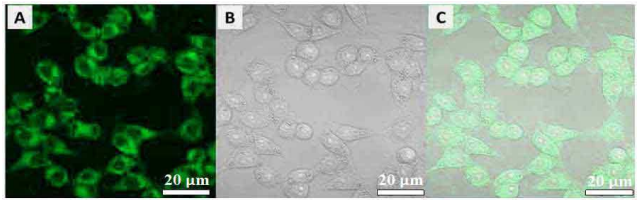

Fig. 5 CLSM images of HeLa cells incubated with 20 μg mL^{-1} of DATPE-poly(PEGMA-co-HEA) LONs for 3 h. (A) cells were excited with a 405 nm laser, (B) Bright fields, (C) merged images of (A) and (B). Scale bar = 20 μm.

Conclusion

In summary, we have explored an interesting strategy for fabrication of AIE active LONs with uniform size, strong fluorescence, great water dispersibility and biocompatibility based on novel AIE dyes and functional polymers. The synthesized polymeric LONs were formed via self assemably of DATPE-poly(PEGMA-co-HEA) copolymers in water. In which the hydrophilic segments were extended into water as the shell while hydrophobic AIE dyes were encapsulated in the core. Beside the stong fluorescence and high water dispersibility, these polymeric LONs could also possess excellent biocompatibility, which make them highly potential for various biomedical applications. As compared with previous strategies, the method described in this work has some advantages. For example, the AIE active polymeric nanoprobes should be more stable than the ones fabricated by noncovalent methods. On the other hand, the pH responsiveness of Schiff base can be used for controlled drug release and possesses better biodegradable potential as compared with the covalent ones. Taken together, we have described a neoteric strategy for fabrication of dynamic cross linked AIE active polymeric nanoprobes, which not only exhibited desirable luminescent properties and dispersibility, but also possessed good biocompatibility and pH responsive properties. These novel AIE active polymeric nanoprobes will provide platforms for fabrication of multifunctional nanosystems with better performance for biomedical applications.

Acknowledgements

This research was supported by the National Science Foundation of China (Nos. 21134004, 21201108, 51363016, 21474057, 21564006, 21561022), and the National 973 Project (Nos. 2011CB935700).

Notes

[a] Department of Chemistry, Nanchang University, 999 Xuefu Avenue, Nanchang 330031, China. [b] Department of Chemistry and the Tsinghua Center for Frontier Polymer Research, Tsinghua University, Beijing, 100084, P. R. China.
xiaoyongzhang1980@gmail.com; weiyen@tsinghua.edu.cn.

† Electronic Supplementary Information (ESI) available: [UV-Vis Spectrum and cell viability of DATPE-poly(PEGMA-co-HEA) LONs et al were provided in supplementary information]. See DOI: 10.1039/b000000x/

References

1. L. Feng, C. Zhu, H. Yuan, L. Liu, F. Lv and S. Wang, *Chem. Soc. Rev.*, 2013, **42**, 6620-6633.
2. R. Hu, N. L. Leung and B. Z. Tang, *Chem. Soc. Rev.*, 2014, **43**, 494-4562.
3. K. Li and B. Liu, *Chem. Soc. Rev.*, 2014, **43**, 6570-6597.
4. A. M. Breul, M. D. Hager and U. S. Schubert, *Chem. Soc. Rev.*, 2013, **42**, 5366-5407.
5. X. Zhang, X. Zhang, S. Wang, M. Liu, L. Tao and Y. Wei, *Nanoscale*, 2013, **5**, 147-150.
6. X. Zhang, K. Wang, M. Liu, X. Zhang, L. Tao, Y. Chen and Y. Wei, *Nanoscale*, 2015, **7**, 11486-11508.
7. K. Wang, X. Zhang, X. Zhang, X. Fan, Z. Huang, Y. Chen and Y. Wei, *Polym. Chem.*, 2015, **6**, 5891-5898.
8. W. Wu, R. Tang, Q. Li and Z. Li, *Chem. Soc. Rev.*, 2015, **12**, 3997-4022.
9. X. Zhang, S. Wang, M. Liu, B. Yang, L. Feng, Y. Ji, L. Tao and Y. Wei, *Phys. Chem. Chem. Phys.*, 2013, **15**, 19013-19018.
10. N. L. Rosi and C. A. Mirkin, *Chem. Rev.*, 2005, **105**, 1547-1562.
11. M. Liu, X. Zhang, B. Yang, Z. Li, F. Deng, Y. Yang, X. Zhang and Y. Wei, *Carbohyd. Polym.*, 2015, **121**, 49-55.
12. X. Zhang, J. Hui, B. Yang, Y. Yang, D. Fan, M. Liu, L. Tao and Y. Wei, *Polym. Chem.*, 2013, **4**, 4120-4125.
13. X. Zhang, S. Wang, C. Zhu, M. Liu, Y. Ji, L. Feng, L. Tao and Y. Wei, *J. Colloid Interf. Sci.*, 2013, **397**, 39-44.
14. X. Zheng, M. Liu, J. Hui, D. Fan, H. Ma, X. Zhang, Y. Wang and Y. Wei, *Phys. Chem. Chem. Phys.*, 2015, **17**, 20301-20307.
15. Q. Zhao, C. Huang and F. Li, *Chem. Soc. Rev.*, 2011, **40**, 2508-2524.
16. J. Zhou, Z. Liu and F. Li, *Chem. Soc. Rev.*, 2012, **41**, 1323-1349.
17. H. S. Choi, W. Liu, P. Misra, E. Tanaka, J. P. Zimmer, B. I. Ipe, M. G. Bawendi and J. V. Frangioni, *Nat. Biotechnol.* , 2007, **25**, 1165-1170.
18. J. Hui, X. Zhang, Z. Zhang, S. Wang, L. Tao, Y. Wei and X. Wang, *Nanoscale*, 2012, **4**, 6967-6970.

19. E. Betzig, G. H. Patterson, R. Sougrat, O. W. Lindwasser, S. Olenych, J. S. Bonifacino, M. W. Davidson, J. Lippincott-Schwartz and H. F. Hess, *Science*, 2006, **313**, 1642-1645.
20. M. Liu, X. Zhang, B. Yang, F. Deng, J. Ji, Y. Yang, Z. Huang, X. Zhang and Y. Wei, *RSC Adv.*, 2014, **4**, 22294-22298.
21. X. Zhang, X. Zhang, L. tao, Z. Chi, J. Xu and Y. Wei, *J. Mater. Chem. B*, 2014, **2**, 4398-4414.
22. K. Li, J. Pan, S. S. Feng, A. W. Wu, K. Y. Pu, Y. Liu and B. Liu, *Adv. Funct. Mater.*, 2009, **19**, 3535-3542.
23. W.-C. Wu, C.-Y. Chen, Y. Tian, S.-H. Jang, Y. Hong, Y. Liu, R. Hu, B. Z. Tang, Y.-T. Lee, C.-T. Chen, W.-C. Chen and A. K.-Y. Jen, *Adv. Funct. Mater.*, 2010, **20**, 1413-1423.
24. X. Zhang, X. Zhang, B. Yang, S. Wang, M. Liu, Y. Zhang and L. Tao, *RSC Adv.*, 2013, **3**, 9633-9636.
25. D. Ding, C. C. Goh, G. Feng, Z. Zhao, J. Liu, R. Liu, N. Tomczak, J. Geng, B. Z. Tang and L. G. Ng, *Adv. Mater.*, 2013, **25**, 6083-6088.
26. J. Luo, Z. Xie, J. W. Y. Lam, L. Cheng, H. Chen, C. Qiu, H. S. Kwok, X. Zhan, Y. Liu, D. Zhu and B. Z. Tang, *Chem. Commun.*, 2001, **37**, 1740-1741.
27. A. Qin, J. W. Lam and B. Z. Tang, *Prog. Polym. Sci.*, 2012, **37**, 182-209.
28. M. Wang, G. Zhang, D. Zhang, D. Zhu and B. Z. Tang, *J. Mater. Chem.*, 2010, **20**, 1858-1867.
29. Z. Li, Y. Q. Dong, J. W. Lam, J. Sun, A. Qin, M. Haußler, Y. P. Dong, H. H. Sung, I. D. Williams and H. S. Kwok, *Adv. Funct. Mater.*, 2009, **19**, 905-917.
30. X. Qi, H. Li, J. W. Y. Lam, X. Yuan, J. Wei, B. Z. Tang and H. Zhang, *Adv. Mater.*, 2012, **24**, 4191-4195.
31. Z. Li, Y. Q. Dong, J. W. Lam, J. Sun, A. Qin, M. Häußler, Y. P. Dong, H. H. Sung, I. D. Williams and H. S. Kwok, *Adv. Funct. Mater.*, 2009, **19**, 905-917.
32. W. Wu, S. Ye, L. Huang, L. Xiao, Y. Fu, Q. Huang, G. Yu, Y. Liu, J. Qin and Q. Li, *J. Mater. Chem.*, 2012, **22**, 6374-6382.
33. X. Zhang, Z. Chi, Y. Zhang, S. Liu and J. Xu, *J. Mater. Chem. C*, 2013, **1**, 3376-3390.
34. Z. Chi, X. Zhang, B. Xu, X. Zhou, C. Ma, Y. Zhang, S. Liu and J. Xu, *Chem. Soc. Rev.*, 2012, **48**, 3878-3896.
35. X. Zhang, M. Liu, B. Yang, X. Zhang, Z. Chi, S. Liu, J. Xu and Y. Wei, *Polym. Chem.*, 2013, **4**, 5060-5064.
36. B. K. An, S. K. Kwon, S. D. Jung and S. Y. Park, *J. Am. Chem. Soc.*, 2002, **124**, 14410-14415.
37. X. Zhang, Z. Ma, M. Liu, X. Zhang, X. Jia and Y. Wei, *Tetrahedron*, 2013, **69**, 10552-10557.
38. C. Saravanan and P. Kannan, *Polym. Degrad. Stabil.*, 2009, **94**, 1001-1012.
39. Z. Wang, B. Xu, L. Zhang, J. Zhang, T. Ma, J. Zhang, X. Fu and W. Tian, *Nanoscale*, 2013, **5**, 2065-2072.
40. X. Zhang, X. Zhang, S. Wang, M. Liu, Y. Zhang, L. Tao and Y. Wei, *ACS Appl. Mater. Interf.*, 2013, **5**, 1943-1947.
41. X. Zhang, X. Zhang, B. Yang, M. Liu, W. Liu, Y. Chen and Y. Wei, *Polym. Chem.*, 2014, **5**, 356-360.
42. M. Liu, X. Zhang, B. Yang, F. Deng, Z. Huang, Y. Yang, Z. Li, X. Zhang and Y. Wei, *RSC Adv.*, 2014, **4**, 35137-35143.
43. M. Liu, X. Zhang, B. Yang, F. Deng, Y. Yang, Z. Li, X. Zhang and Y. Wei, *Macromol. Biosci.*, 2014, **14**, 1712-1718.
44. M. Liu, X. Zhang, B. Yang, L. Liu, F. Deng, X. Zhang and Y. Wei, *Macromol. Biosci.*, 2014, **14**, 1260-1267.
45. Y. Liu, X. Feng, J.-g. Zhi and B. Tong, *Chin. J. Polym. Sci.*, 2012, **30**, 443-450.
46. X. Zhang, X. Zhang, B. Yang and Y. Wei, *Chin. J. Polym. Sci.*, 2014, **32**, 871-879.
47. X. Zhang, X. Zhang, B. Yang, J. Hui, M. Liu, W. Liu, Y. Chen and Y. Wei, *Polym. Chem.*, 2014, **5**, 689-693.
48. X. Zhang, X. Zhang, B. Yang, M. Liu, W. Liu, Y. Chen and Y. Wei, *Polym. Chem.*, 2013, **4**, 4317-4321.
49. X. Zhang, X. Zhang, B. Yang, M. Liu, W. Liu, Y. Chen and Y. Wei, *Polym. Chem.*, 2014, **5**, 399-404.
50. H. Shi, R. T. Kwok, J. Liu, B. Xing, B. Z. Tang and B. Liu, *J. Am. Chem. Soc.*, 2012, **134**, 17972-17981.
51. H. Shi, J. Liu, J. Geng, B. Z. Tang and B. Liu, *J. Am. Chem. Soc.*, 2012, **134**, 9569-9572.
52. Z. Wang, S. Chen, J. W. Lam, W. Qin, R. T. Kwok, N. Xie, Q. Hu and B. Z. Tang, *J. Am. Chem. Soc.*, 2013, **135**, 8238-8245.
53. Z. Huang, X. Zhang, X. Zhang, B. Yang, Y. Zhang, K. Wang, J. Yuan, L. Tao and Y. Wei, *Polym. Chem.*, 2015, **6**, 2133-2138.
54. Z. Huang, X. Zhang, X. Zhang, C. Fu, K. Wang, J. Yuan, L. Tao and Y. Wei, *Polym. Chem.*, 2015, **6**, 607-612.
55. C.-Y. Chen, T. H. Kim, W.-C. Wu, C.-M. Huang, H. Wei, C. W. Mount, Y. Tian, S.-H. Jang, S. H. Pun and A. K.-Y. Jen, *Biomaterials*, 2013, **34**, 4501-4509.
56. Q. Lv, K. Wang, D. Xu, M. Liu, Q. Wan, H. Huang, S. Liang, X. Zhang and Y. Wei, *Macromol. Biosci.*, DOI: 10.1002/mabi.201500256.
57. H. Li, X. Zhang, X. Zhang, K. Wang, H. Liu and Y. Wei, *ACS Appl. Mater. Interf.*, 2015, **7**, 4241-4246.
58. Q. Wan, K. Wang, H. Du, H. Huang, M. Liu, F. Deng, Y. Dai, X. Zhang and Y. Wei, *Polym. Chem.*, 2015, **6**, 5288-5294.
59. X. Zhang, H. Qi, S. Wang, L. Feng, Y. Ji, L. Tao, S. Li and Y. Wei, *Toxicol. Res.*, 2012, **1**, 201-205.
60. X. Zhang, S. Wang, M. Liu, J. Hui, B. Yang, L. Tao and Y. Wei, *Toxicol. Res.*, 2013, **2**, 335-346.
61. A. Bajpai, S. K. Shukla, S. Bhanu and S. Kankane, *Prog. Polym. Sci.*, 2008, **33**, 1088-1118.
62. Y. Xin and J. Yuan, *Polym. Chem.*, 2012, **3**, 3045-3055.
63. X. Zhang, J. Yin, C. Peng, W. Hu, Z. Zhu, W. Li, C. Fan and Q. Huang, *Carbon*, 2011, **49**, 986-995.
64. X. Zhang, J. Yin, C. Kang, J. Li, Y. Zhu, W. Li, Q. Huang and Z. Zhu, *Toxicol. Lett.*, 2010, **198**, 237-243.
65. X. Zhang, Y. Zhu, J. Li, Z. Zhu, J. Li, W. Li and Q. Huang, *J. Nanopart. Res.*, 2011, **13**, 6941-6952.
66. X. Zhang, W. Hu, J. Li, L. Tao and Y. Wei, *Toxicol. Res.*, 2012, **1**, 62-68.

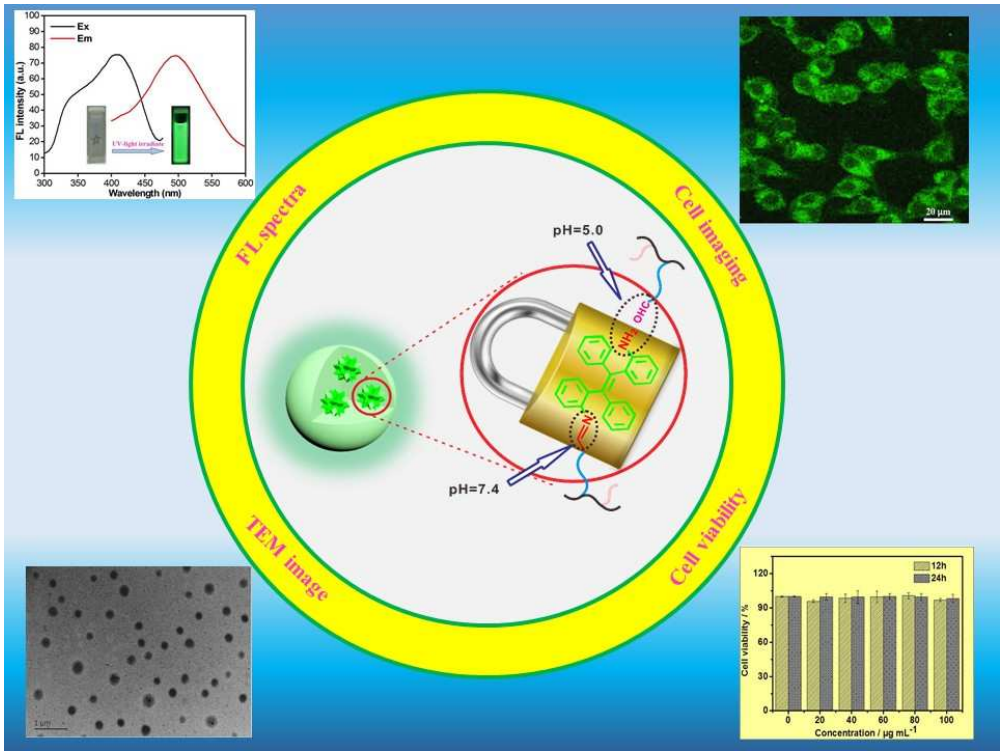

Stumuli responsive AIE-active polymeric luminescent nanoprobes have been fabricated through formation of dynamic bonds using AIE dye as the linker